The following publication L. Ding and C. K. Tse, "Large-Signal Stability Analysis of DC Distribution Systems With Cascading Converter Structure," in IEEE Transactions on Industrial Electronics, vol. 70, no. 9, pp. 9103-9111, Sept. 2023 is available at https://doi.org/10.1109/TIE.2022.3206692.

Large-Signal Stability Analysis of DC Distribution Systems with Cascading Converter Structure

Li Ding, *Student Member, IEEE*, Chi K. Tse, *Fellow, IEEE*

***Abstract*—DC-DC converters are major components of the DC distribution systems. The converters interface with external power inputs, internal DC buses and loadings of subsystems. The interfacing DC-DC converters should be stable locally and globally under mutual interactions through a DC bus within the system. Current research efforts have focused on the analysis of the stability of the DC distribution system subject to small-signal disturbance. However, in practice, the system routinely operates under large-signal disturbances, such as when an additional subsystem is turned on after being connected to the DC bus. In this scenario, the small-signal model may fail to fully describe the dynamics of the system. In this paper, we identify and analyze the bifurcation process when the system undergoes abrupt load changes. According to the nonlinear operation of the interconnected system, a large-signal stability criterion is derived. This criterion is simple, and can be easily extended to multiple connected converter systems. The criterion is also consistent with the result from bifurcation analysis. Finally, the validity of the proposed criterion is verified by the full-circuit simulations and the experimental works.**

***Index Terms*—Bifurcation analysis, constant power load, DC distribution system, design-oriented analysis, large-signal disturbance, stability criterion**

I. Introduction

DC distribution systems are widely used in micro-grids, electric vehicles, communication systems and other power supply applications [1]–[3]. Within a DC distribution system, power sources and loads are connected with interfacing power converters via a DC bus. In this system, interacting power converters should be designed for a stable operation according to some system design criteria [4]–[6].

The stability criteria of DC distribution systems can be derived from small-signal and large-signal points of view. For the small-signal stability analysis, the first criterion was proposed by Middlebrook in 1976 [7] for a DC cascaded system which is the ancestor of today's micro-grid system. According to Middlebrook's criterion, the stability of a system of two DC-DC converters in cascaded connection can be guaranteed if both the source converter and the load converter are stable individually and the magnitude of the output impedance of the source converter is smaller than the magnitude of the input impedance of the load converter within the entire frequency range. Subsequently, many impedance based criteria [8]–[12] have been developed aiming to narrow the forbidden range given by Middlebrook's criterion and increase the degree of freedom of a design.

The above impedance-based criteria are derived from the small-signal stability analysis, which permits fast calculation, but can be inaccurate for large-signal operations. Therefore, some large-signal analysis methods have been proposed. The behavior of a DC cascaded system under large-signal disturbance has been described and analyzed by phase-plane analysis [13]–[15]. In these previous works, the system's differential equations are graphically solved (plotted), providing the trajectories on the phase plane. Specifically, the graphical and experimental results show that the DC bus voltage and the output voltage of the system may collapse under sudden load changes. The phase-plane analysis is explicit and suitable for numerical simulations. However, detailed internal parameters should be specified and different parameters produce different trajectories. Also, it does not readily generate an analytical and general relationship between the parameters and the system's stability.

Apart from the phase-plane analysis, Lyapunov-based methods are the effective and widely used to analyze the large-signal stability of the system. In reference [16], the stability of a three-phase two-level power converter under different time scales has been analyzed based on the Lyapunov function. The Lyapunov stability theorem is also applied to the DC-DC converters to obtain the stability of global asymptotic conditions [17].

However, for more complex power electronics systems, it is difficult to find the Lyapunov function. Some methods, such as the Takagi-Sugeno multi-modeling [18] and Brayton-Moser's mixed potential function theory [19], have been developed to generate the Lyapunov function. The Brayton-Moser mixed potential function theory can be used to analyze the large-signal stability of the nonlinear circuits and obtain the analytical solution of the stable operating region [20]. In reference [21], a large-signal stability criterion has been derived with mixed potential theory to analyze the catastrophic bifurcation phenomenon of the photovoltaic-battery hybrid power system under large-signal disturbance. In reference [22], based on an equivalent gyrator model of the buck converter, a criterion derived from the mixed potential theory has been used to study the large-signal stability of a current-mode controlled

Manuscript received Month xx, 2022; revised Month xx, xxxx; accepted Month x, xxxx. This work is supported by Hong Kong Research Grant Council under GRF 112071/21E.

L. Ding is with the Department of Electronic and Information Engineering, The Hong Kong Polytechnic University, Hunghom, Hong Kong. (Email: kenny.ding@connect.polyu.hk).

C. K. Tse is with the Department of Electrical Engineering, City University of Hong Kong, Kowloon, Hong Kong. (Email: cktse@ieee.org).

DC cascaded system. The results of these two prior works show that the output voltage of the source converter gets close to the load converter's output voltage under transient disturbance which is generated by stepping up the load from almost no load to full load in a very short time. In reference [23], the mixed potential function of a DC system cascaded with a LC filter and a constant power load has been established to analyze the effect of different control parameters on the large-signal stability of the system. However, again, detailed internal parameters are needed when applying the mixed potential function theory and this method involves tedious computation and is difficult to apply to the DC distribution systems containing a number of subsystems. Therefore, it is highly desirable to have a simple and effective criterion to investigate the large-signal stability of the DC distribution system from a design-oriented perspective.

In this paper, we study the bifurcation phenomenon and derived a stability criterion for practical designs. The focus of this study is to identify the instability conditions and the stability boundaries of the system under an abrupt load change situation. A simple and effective criterion is proposed to analyze the transient behaviors and to give the stability boundaries of the system. The results will be presented in design-oriented forms that can facilitate the choice of parameters for ensuring the system's stable operation.

This paper is organized as follows. The instability of the system from a bifurcation viewpoint and the physical origin of the phenomenon are exposed in Section II. By showing this instability mechanism, a large-signal criterion based on the steady operating point is developed in Section III. The criterion is generated directly from the bifurcation analysis and an extension of the criterion to the DC distribution systems containing a number of subsystems will also be shown. A theoretical analysis of the stability boundary of the system is given. Section IV experimentally verifies the analysis. Finally, Section V concludes this paper.

II. Bifurcation Phenomenon and Analysis

A typical structure of a DC distribution system with one source converter (B_s) and two load converters (B_1 and B_2) is shown in Fig. 1. For illustrative purposes, both B_1 and B_s are buck converters and B_2 is a boost converter, but the analysis method can be extended to any other types of converters. In this system, the bus voltage is regulated by B_s. All converters are controlled with three independent voltage-mode controller circuits, as shown in Fig. 2. The maximum duty cycle of these three converters are clamped at 0.9. The power source E shown in Fig. 1 is 24 V. Also, $r_{\rm Line} = 0.6\ \Omega$ and $L_{\rm Line} = 5\ \mu$H account for the wire impedance from the source converter to load converters. The values of the circuit components used in the full circuit simulation are given in Table I, where $g = R_a/R_f$, $\tau = R_aC_a$ and $K_v = R_d/(R_d + R_c)$. In the following sections, the subscripts $1, 2$ and s in the symbols are used to represent B_1, B_2 and B_s, respectively.

A. Bifurcation Phenomenon

In practice, the source converter and the load converters are decentralized in a DC distribution system and the load

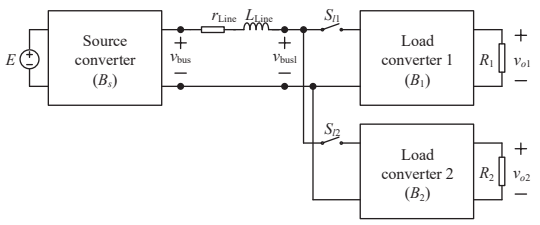

Fig. 1. DC distributed system with a source converter and two load converters.

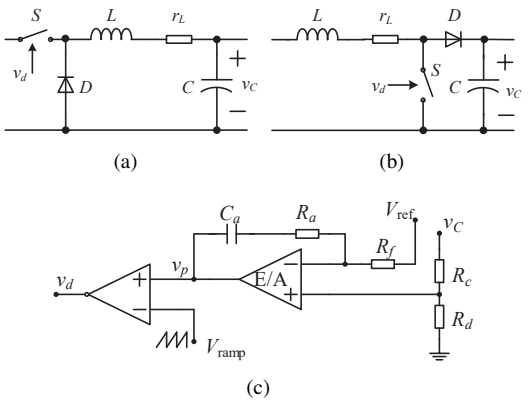

Fig. 2. (a) Buck converter circuit, for building the load converter 1 (B_1) and the source converter (B_s); (b) boost converter, for building the load converter 2 (B_2); (c) controller circuit of B_1, B_2 and B_s.

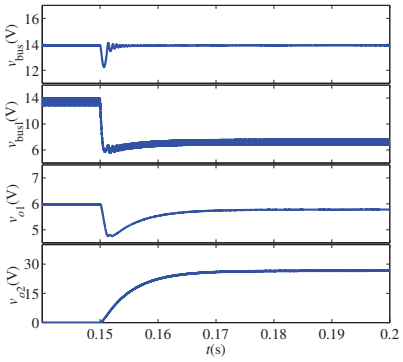

Fig. 3. Voltage collapse on the input port of the load converters and the output voltage of B_1 after B_2 is connected to the DC bus.

TABLE I
Circuit Components

Component	B_1	B_2	B_s	Component	B_1	B_2	B_s
L / μH	470	220	220	g	19.6	0.02	19.6
C / μF	680	680	680	τ / s	0.1	0.1	0.01
r_L / Ω	0.5	0.5	0.5	K_v	0.84	0.17	0.36
R / Ω	6	30	–	$V_{\rm ref}$ / V	5	5	5
v_C / V	6	30	14	f / kHz	16	16	16

converters may not connect to the DC bus at the same time. Without loss of generality, we assume that S_{l1} is turned on before $t = 0$ s, which means that source converter B_s and load converters B_1 are stable. After $t = 0.15$ s, S_{l2} is turned on and B_2 is connected to the DC bus.

Fig. 3 shows the transient waveforms of the system when S_{l2} is turned on some time after S_{l1} is turned on. After B_2 is connected to the DC bus, it can be observed that the input voltage of the load converters ($v_{\rm busl}$) drops to 7 V. This voltage drop will also make the voltage input to B_1 and B_2 a bit lower or even to a point lower than the required output of B_1 and B_2. So, the output voltage of B_1 drops to less than 6 V, and the output voltage of B_2 cannot reach its desired output value which is 30 V. The instability is irreversible, and the system is stuck in the abnormal state.

B. Bifurcation Analysis

In general, bifurcations can be classified into continuous and discontinuous bifurcations, depending on whether the states of the system are varying continuously or discontinuously. The cause of this bifurcation is that there is a structural change in the system as the parameters of the system are varied through the critical point, and such a bifurcation may cause undesirable or even catastrophic consequences as the state variables may exhibit undesirably wide excursion in the state space causing damage to some system components [24].

As shown in Fig. 3, when B_2 is connected to the DC bus, the system becomes unstable. The input voltage of the load converters collapses, and excessive power is consumed by the wire resistor. The output voltage of the load converters fall below the desired values. Meanwhile, the duty cycles of the load converters are fixed at the maximum values, which cause high current stress on the switching devices.

When a load converter is plugged to the DC bus, there is a large-signal disturbance on the dc bus line. In order to investigate the bifurcation phenomenon of the system during the transient, the discrete-time mapping model has to be established. In this system, all the subsystems are designed for operation in continuous conduction mode (CCM). A state vector $\mathbf{x}$ containing three 3-dim column vectors $\mathbf{x}_s$, $\mathbf{x}_1$ and $\mathbf{x}_2$ for converters B_s, B_1 and B_2, respectively, is chosen as follows:

$$\mathbf{x} = \left[\mathbf{x}_s\ \mathbf{x}_1\ \mathbf{x}_2\right]^T, \tag{1}$$

where

$$\begin{aligned} \mathbf{x}_s &= \left[i_{Ls}\ v_{Cs}\ v_{as}\right]^T, \\ \mathbf{x}_1 &= \left[i_{L1}\ v_{C1}\ v_{a1}\right]^T, \\ \mathbf{x}_2 &= \left[i_{L2}\ v_{C2}\ v_{a2}\right]^T. \end{aligned} \tag{2}$$

Without loss of generality, we can assume that the subsystems share and synchronize a common period T, having eight operating states as described in Table II. The state-j equation, where $j = 1, 2, 3, 4, 5, 6, 7, 8$, within a period is given by

$$\dot{\mathbf{x}} = \mathbf{A}_j\mathbf{x} + \mathbf{B}_j E \qquad \text{state } j. \tag{3}$$

Expressions of $\mathbf{A}_j$ and $\mathbf{B}_j$ can be readily found and are omitted here.

TABLE II
CIRCUIT OPERATING STATES

State	S_s	D_s	S_1	D_1	S_2	D_2
1	off	on	off	on	off	on
2	off	on	off	on	on	off
3	off	on	on	off	off	on
4	off	on	on	off	on	off
5	on	off	off	on	off	on
6	on	off	off	on	on	off
7	on	off	on	off	off	on
8	on	off	on	off	on	off

Then, the discrete-time model that describes the dynamics of the system can be derived from equation (3). Suppose the switching period is T. Denote $\mathbf{x}(nT) = \mathbf{x}_n(0)$, or simply $\mathbf{x}_n$ for brevity, which is the initial value at the beginning of switching period n. Within a period T, the state-j equation given by (3) describes the system starting from time $(nT + \tau_{j-1})$ to $(nT+\tau_j)$ for a time interval of $T_j = \tau_j - \tau_{j-1}$, where $\tau_0 = 0$ and $\tau_8 = T$, such that $\sum_j T_j = T$. Using equation (3), the value of $\mathbf{x}_n(\tau_j)$ by the end of this state-j is given by:

$$\mathbf{x}_n(\tau_j) = \mathbf{N}_j\left(T_j\right)\mathbf{x}_n(\tau_{j-1}) + \left(\mathbf{N}_j\left(T_j\right) - \mathbf{I}\right)\mathbf{A}_j^{-1}\mathbf{B}_j E, \tag{4}$$

where $\mathbf{I}$ is an 9×9 identity matrix, and $\mathbf{N}_j(\xi)$ is the corresponding system matrices given by

$$\mathbf{N}_j(\xi) = e^{\mathbf{A}_j\xi} = \mathbf{I} + \sum_{k=1}^{\infty}\frac{1}{k!}\mathbf{A}_j^k\xi^k. \tag{5}$$

Equation (4) can be rewritten as $\mathbf{x}_n(\tau_j) = f_j(\mathbf{x}_n(\tau_{j-1}))$. In this way, $\mathbf{x}_{n+1} = \mathbf{x}_n(T) = \mathbf{x}_n(\tau_8)$ can be determined iteratively from $\mathbf{x}_n(0) = \mathbf{x}_n$ using equation (4). Thus, in general, we have

$$\mathbf{x}_{n+1} = \mathbf{f}(\mathbf{x_n}). \tag{6}$$

To complete the derivation, we have to find the relation among the duty cycles of the subsystems and the state variables $\mathbf{x}_n$. According to Fig. 2, switch S_i will be turned off when $s_i\left(\mathbf{x}_n\ d_{in}\right) \triangleq \left(v_{pi} - v_{{\rm ramp}i}\right)$ is zero as:

$$s\left(\mathbf{x}_n\ d_n\right) \triangleq v_{\rm p} - v_{\rm ramp} = 0. \tag{7}$$

The equilibrium point $\mathbf{X}_Q$ and the corresponding duty cycle D_Q of the system can be found by determining the steady-state solutions. Using the discrete-time model developed earlier, the steady-state variables and the duty cycles can be found by putting $\mathbf{x}_{n+1} = \mathbf{x}_n = \mathbf{X}_Q$ and $d_n = D_Q$. In the steady state, the capacitor voltages equal the bus voltage and the output of the system, i.e., $V_{Cs} = V_{bus}$, $V_{C1} = V_{o1}$ and $V_{C2} = V_{o2}$. Defining

$$\mathbf{X}_Q = \left[I_{Ls}\ V_{bus}\ V_{As}\ I_{L1}\ V_{o1}\ V_{A1}\ I_{L2}\ V_{o2}\ V_{A2}\right]^T, \tag{8}$$

and solving for $\mathbf{X}_Q$ and D_Q, we get

$$V_{oi} = k_{di} V_{\mathrm{ref}i}, \tag{9a}$$
$$V_{\mathrm{bus}} = k_{ds} V_{\mathrm{ref}s}, \tag{9b}$$
$$I_{Ls} = \frac{V_{\mathrm{bus}} - \sqrt{V_{\mathrm{bus}}^2 - 4Pr_{\mathrm{Line}}}}{2r_{\mathrm{Line}}}, \tag{9c}$$
$$V_{\mathrm{busl}} = V_{\mathrm{bus}} - I_{Ls} r_{\mathrm{Line}}, \tag{9d}$$
$$D_{Qs} = \frac{V_{\mathrm{bus}}}{E}, \tag{9e}$$
$$I_{L1} = \frac{V_{o1}}{R_1}, \tag{9f}$$
$$D_{Q1} = \frac{V_{o1}\left(1 + \frac{r_{L1}}{R_1}\right)}{V_{\mathrm{busl}}}, \tag{9g}$$
$$I_{L2} = \frac{V_{o2}}{R_2\left(1 - D_{Q2}\right)}, \tag{9h}$$
$$D_{Q2} = \frac{1 - \left(b + \sqrt{b^2 - 4c}\right)}{2}, \tag{9i}$$
$$V_{As} = V_{\mathrm{ref}s} - (1 - D_{Qs}) V_{\mathrm{ramp}s}, \tag{9j}$$
$$V_{Ai} = V_{\mathrm{ref}i} - (1 - D_{Qi}) V_{\mathrm{ramp}i}, \tag{9k}$$

where $b = \frac{V_{\mathrm{busl}}}{V_{o2}}$, $c = \frac{r_{L2}}{R_2}$, $P = \frac{V_{o1}^2}{R_1} + \frac{V_{o2}^2}{R_2}$, $i = 1, 2$.

The dynamics of the system in a small neighborhood of the equilibrium point or orbit can be inspected by determining the eigenvalues of the Jacobian of the system. Then, by varying some selected system parameters and tracking the movement of the eigenvalues, the stability information such as the bifurcation point and the boundaries of operating regions can be identified. The Jacobian matrix can be derived from the state equations and by perturbing around the equilibrium point, and then the eigenvalues can be calculated by solving λ in the characteristic equation given by:

$$\det\left[\lambda \mathbf{I} - J\left(\mathbf{X}_Q\right)\right] = 0. \tag{10}$$

From equation (10), we can get all the eigenvalues of the Jacobian matrix. From Figs. 5(a) and (b), it can be found that all the eigenvalues are inside the unit circle before B_2 is connected to the DC bus, which means that the system is in the stable operating region. After B_2 is connected to the DC bus, an eigenvalue touches the unit circle on the positive real line while other eigenvalues stay in the unit circle, as shown in Figs. 4(c) and (d). This means that a saddle-node bifurcation occurs.

The saddle-node bifurcation results in the creation of a new orbit (or the destruction of an existing orbit). In this system, after B_2 is connected to the DC bus, v_{o1} drops and cannot be recovered to the original value. Meanwhile, v_{o2} is fixed at the value that is lower than the desired value. The phenomenon can be seen more clearly in the phase portrait, as shown in Figs. 5(a) and (b). After B_2 is connected, the trajectory of B_1 fails to converge to its original desired operating point while the trajectory of B_2 cannot reach its desired operating point and stays at the abnormal state finally. This means that both B_1 and B_2 operate in the new orbits which are not in the desired operating region. This result agrees with the full-circuit simulation results provided in Fig. 3 that the output voltage of B_1 collapses after B_2 is connected to the DC bus and the output voltage of B_2 cannot reach its desired value.

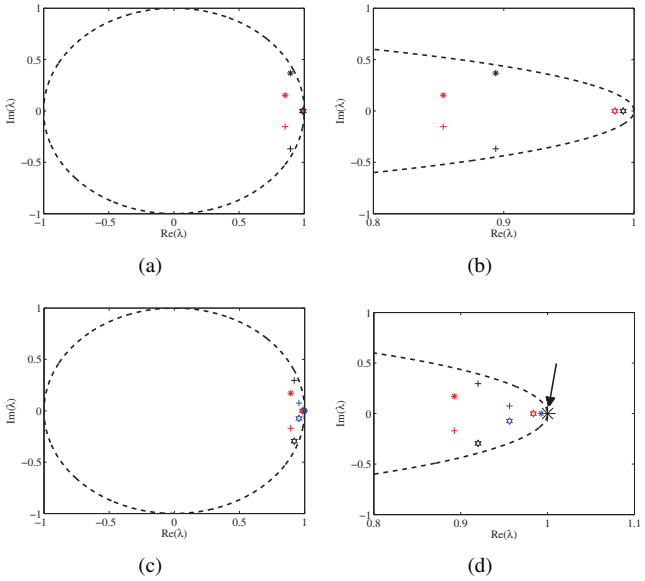

Fig. 4. Movement of the eigenvalues when bifurcation occurs. (a) Before B_2 is added to the DC bus; (b) enlargement of (a); (c) after B_2 is added to the DC bus; (d) enlargement of (c).

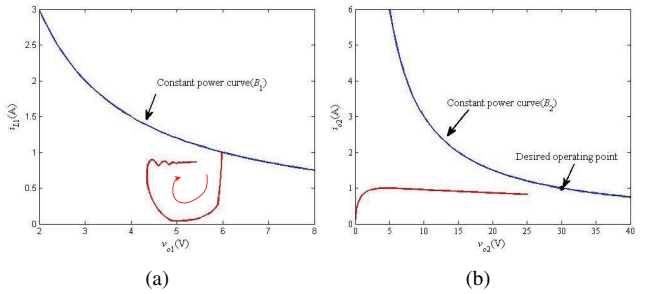

Fig. 5. Phase portrait views of the saddle-node bifurcation after B_2 is connected to the DC bus. (a) Blue curve: constant power curve of B_1; red curve: phase portrait of B_1; (b) blue curve: constant power curve of B_2; red curve: phase portrait of B_2.

III. Large-Signal Stability Criterion

A. Revisit the System's Transition under Large-Signal Disturbance

In order to derive the large-signal stability criterion, it is important to revisit the system's dynamic behavior when B_2 is connected to the DC bus. After $t = 0.15$ s, S_{l2} is turned on and B_2 is connected to the DC bus. Since the load converters are connected in parallel, the connection of B_2 will cause a drop of the overall input impedance of the load converters. Due to the presence of the line impedance, the drop in the overall input impedance of the load converters will lead to a voltage drop at the input port of the load converters. After being connected to the DC bus, B_2 is in a start-up process. During the start-up process, the controller of B_2 initially saturates the duty cycle at its maximum value for fast reaching of the controller's

reference value. Meanwhile, B_1 may enter the accommodation region since the a voltage drop occurs in $v_{\rm busl}$.

From the foregoing discussion and the previous full-circuit simulation results, we can see that there is a complex interaction among the subsystems through the non-ideal DC bus when the DC distribution system is under large-signal disturbance such as an abrupt load change, and such disturbance may cause the voltage of the DC bus to collapse and thus would affect the stability of the whole system. Meanwhile, the collapse of the bus voltage may cause undesirable or even catastrophic consequences as the current magnitude on the DC bus have a sudden increase which may damage the system's components.

B. Stable Operation Requirements of the System

If the system can maintain stability under large-signal disturbance, it can finally return to the desired operating point. For this case, B_2 can start-up successfully and B_1 can recover to its normal operating state. This also means that all the load converters can maintain a constant power load (CPL) characteristic. Since all the load converters have a duty cycle limit (D_m), in order to ensure the load converters maintaining the CPL characteristic, the duty cycle should always lie within the range (0, D_m). Thus, the input voltage of each load converter should be greater than a permissible minimum value to ensure that the system can return to the desired operating point. Otherwise, the duty cycle will saturate and stay at D_m, and the load converters will operate in an open-loop condition and behave as resistive loads rather than CPLs.

C. Concept of the Criterion

From the foregoing discussion, it can be concluded that the input voltage of the load converters can be used as an indicator to assess the large-signal stability of the system. Here, only the steady-state values need to be considered and the detailed dynamics such as oscillation can be ignored. This is because the load converters may fail to maintain the CPL characteristic and can be judged operating in an undesired region if their input voltages are below the permissible minimum value. Thus, it is reasonable to derive a criterion using a set of algebraic equations instead of differential equations to investigate the system's stability under large-signal disturbance.

It should be pointed that under an abrupt load change situation, the duty cycle of a load converter which was stable originally, e.g., B_1, may not reach the maximum value during the accommodation process. This is because the initial value of the energy storage element is not zero if the converter is stable originally. However, for simplification, we will consider the critical condition corresponding to all the load converters operating at the maximum duty cycle during the adjusting transition.

D. Derivation of the Criterion

When B_1 and B_2 operate in the critical condition, the relation of the output voltages and the converter's parameters in the steady state can be defined as

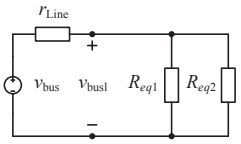

Fig. 6. Equivalent circuit of the system under large-signal disturbance.

$$V_{\rm busl1} = V_{o1}(R_1 + r_{L1})/(D_{m1}R_1). \tag{11}$$

$$V_{\rm busl2} = V_{o2}[(1 - D_{m2})^2 R_2 + r_{L2}]/((1 - D_{m2})R_2). \tag{12}$$

Here, D_{m1} and D_{m2} represent the maximum duty cycle values of B_1 and B_2, respectively. $V_{\rm busl1}$ and $V_{\rm busl2}$ represent the permissible minimum input voltage values of B_1 and B_2, respectively. For simplicity, only the equivalent series resistances of the inductors are taken into account, with other parasitic parameters such as equivalent series resistances of the capacitors all set to zero. Detailed derivation of the equations (11) and (12) can be found in a prior work [25].

From the foregoing discussion, the steady-state value of the load converters' input voltage is adopted to inspect the large-signal stability of the system. Thus, it is important to analyze the allocation of $V_{\rm bus}$ on the wire impedance and the input port of the load converters.

Under the critical condition, the whole system can be simplified as shown in Fig. 6. In this model, B_s is equivalent to a voltage source, and $V_{\rm bus}$ is the output voltage of B_s. Equivalent resistances R_{eq1} and R_{eq2} are the DC values of input resistances of the load converters which are operating at their maximum duty cycles. Here, the line inductance is not included in the simplified model. The reason is that the it only affects the dynamic of the system, and have no effect on the calculation of the steady-state operating point of the system.

According to equations (11) and (12), each load converter has its permissible minimum input voltage because the output voltages of the load converters are different. Since the load converters are in parallel connection, an overall permissible minimum input voltage $V_{\rm busl\,min}$ should be greater than the biggest one. Thus, $V_{\rm busl\,min}$ is defined as

$$V_{\rm busl\,min} \geq \max\left\{V_{\rm busl1},\, V_{\rm busl2}\right\}. \tag{13}$$

According to Fig. 5 and equations (11), (12) and (13), the large-signal stability criterion can be given as:

$$\begin{aligned} V_{\rm busl\,min} &= \frac{R_{eq} v_{\rm bus}}{R_{eq} + r_{\rm Line}} \\ &\geq \max\left\{\frac{V_{o1} D_{m1} R_{eq1}}{R_1}, \frac{V_{o2} R_{eq2}}{(1 - D_{m2})R_2}\right\}. \end{aligned} \tag{14}$$

Here $R_{eq} = R_{eq1} || R_{eq2}$; and $R_{eq1} = \frac{R_1 + r_{L1}}{D_{m1}^2}$ and $R_{eq2} = (1 - D_{m2})^2 R_2 + r_{L2}$ represent the DC values of the input impedances of B_1 and B_2, respectively. It is obviously that the parameters used to calculate the boundary of the system are the load, equivalent series resistance of the inductor, output voltage and the maximum duty cycle of each load converter,

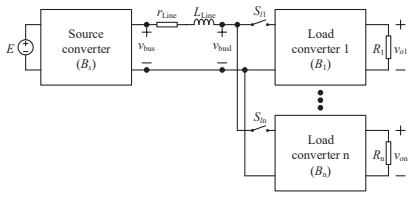

Fig. 7. DC distributed system with one source converter and multi-load converters.

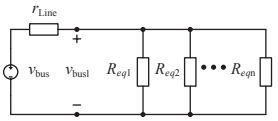

Fig. 8. Equivalent circuit of the system under large-signal disturbance (N load converters).

which are easy to obtain. Since the subsystems interact with each other under large-signal disturbance through the line resistance which is normally omitted, the stability threshold (boundary) of $r_{\rm Line}$ should be investigated. Substituting the parameters given in Table I into inequality (14), we get $r_{\rm Line} \leq \min\{0.68\ \Omega, 0.54\ \Omega\}$. Hence, if $r_{\rm Line}$ is greater than 0.54 Ω, the system will lose stability under large-signal disturbance. The analysis result based on the derived criterion agrees with the previous full-circuit simulation result and the bifurcation analysis result.

E. Extension of the Criterion to the Large-Scale DC Distribution Power System

From the previous discussion, it can be found that the parameters used in the criterion are easily obtained and the calculation process is simple. So, the stability criterion can be easily extended to the system containing a number of subsystems. Fig. 7 is a representative DC distribution system consisting of one source converter which regulates the bus voltage and a number of load converters, each of which regulates its own output. Without loss of generality, we assume that all the switches except S_{ln} are turned on before $t = 0$ s, which means that the source converter B_s and the load converters B_1 to B_{n-1} have already operated stable. After $t = 0$ s, S_{ln} is turned on and B_n is connected to the DC bus. According to the previous discussion, if v_{busl} can be guaranteed to be greater than the permissible minimum input voltage, the whole system can keep stable after the abrupt load change situation and permissible minimum input voltage of this system can be derived as follow:

$$V_{{\rm busl}i} = f(D_{mi},\, V_{oi},\, R_i,\, r_{Li}), \tag{15}$$

where V_o, D_m, R, r_L and $V_{\rm busl}$ represent the steady-state values of output voltage, maximum duty cycle value, load, equivalent series resistance of the inductor and the permissible minimum input voltage, respectively. Also, $i = 1, ...n$ denotes load converters B_1 to B_n.

When the system operates in critical condition, where all the load converters operate at their maximum duty cycles, the whole system can be simplified, as shown in Fig. 8.

Here, equivalent resistances R_{eq1} to R_{eqn} are the input resistances of the load converters which are operating at their maximum duty cycles. Since each load converter has its permissible minimum input voltage $V_{{\rm busl}i}$ because the output voltages of the load converters are different. In addition, because the load converters are in parallel connection, thus, the overall permissible minimum input voltage $V_{\rm busl\,min}$ should be greater than the largest one of $V_{{\rm busl}i}$. So, $V_{\rm busl\,min}$ is defined as

$$V_{\rm busl\,min} \geq \max\left\{V_{\rm busl1},\, V_{\rm busl2} \cdots V_{{\rm busl}i}\right\}. \tag{16}$$

According to the previous discussion and Fig. 8, the large-signal stability criterion of the system under large-signal disturbance can be expressed as

$$V_{\rm busl\,min} = \frac{R_{eq} V_{\rm bus}}{R_{eq} + r_{\rm Line}} \geq \max\left\{V_{\rm busl1}, V_{\rm busl2} \cdots V_{{\rm busl}i}\right\}, \tag{17}$$

where $R_{eq} = 1/\sum_{i=1}^{n}(1/R_{eqi})$.

F. Description of the Effect of the Soft-Start Routine on the System's Stability

In practice, a soft-start routine is usually incorporated in the control. Also, the effect of the soft-start routine on the system's stability under large-signal disturbance has been rarely reported in prior works. Therefore, the effect of the soft-start routine on the proposed criterion will be discussed in this subsection.

Fig. 9 shows the relationship between the maximum duty cycle value of B_2 and the stability boundary of $r_{\rm Line}$. In the previous discussions, B_2 is a hard switching converter, and we assume that the duty cycle of B_2 will fix at D_{m2} during the whole start-up process after it is connected to the DC bus. If the soft-start routine is introduced, the duty cycle of B_2 will increase gradually from 0 to D_{m2} instead of increasing to and keeping at D_{m2} rapidly in the transient process. Therefore, the value of the equivalent duty cycle of B_2 in the start-up process is smaller than that in hard switching case. Here, the equivalent duty cycle of B_2 can be regarded as the averaged value of the duty cycle in the start-up process and can be used to replace D_{m2} in inequality (14) to obtain the boundary of the system under large-signal disturbance.

From Fig. 9, it can be observed that the stability boundary of the system may vary with the maximum duty cycle of B_2. By adjusting the soft-start parameters and making the equivalent duty cycle of B_2 in the start-up process equals 0.79, and using this value to calculate the boundary through inequality (14), $r_{\rm Line}$ reaches the peak value, and the system can become stable under large-signal disturbance when $r_{\rm Line} \leq 0.91\ \Omega$. However, if we further increase the soft-start duration, which means that the value of the equivalent duty cycle of B_2 in the start-up process is further decreased, the maximum value of $r_{\rm Line}$ will decrease, which means that it will narrow the stability boundary of the system.a long soft-start duration may lead a poor transient performance of the system.

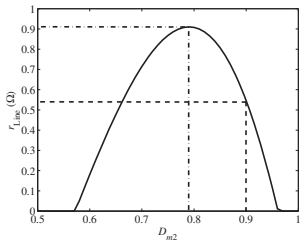

Fig. 9. Relationship between D_{m2} and r_{Line}.

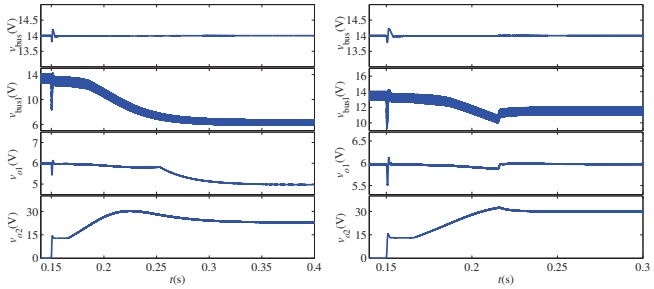

(a) (b)

Fig. 10. Transient waveforms (a) for $r_{\mathrm{Line}} = 1\ \Omega$ (with soft-start), showing unstable system under large-signal disturbance; (b) for $r_{\mathrm{Line}} = 0.8\ \Omega$ (with soft-start), showing stable system under large-signal disturbance.

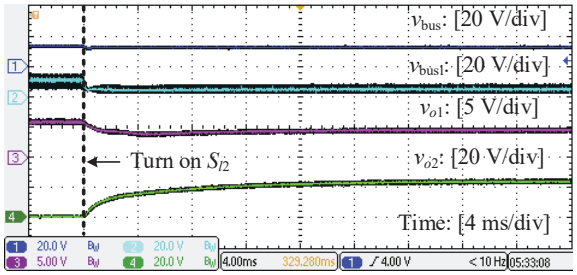

(a)

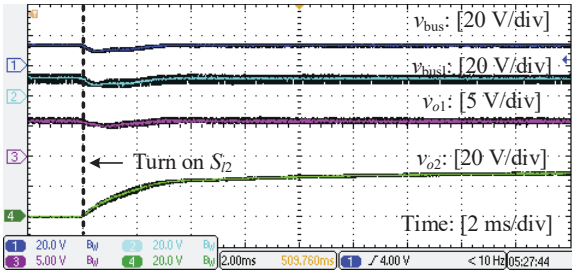

(b)

Fig. 11. Transient waveforms (a) for $r_{\mathrm{Line}} = 0.6\ \Omega$ (without soft-start), showing unstable system under large-signal disturbance; (b) for $r_{\mathrm{Line}} = 0.5\ \Omega$ (without soft-start), showing stable system under large-signal disturbance.

A long soft-start duration may lead a poor transient performance of the system. So, in practice, the soft-start time is in the range of 25 to 100 switching cycles [26], which is smaller than the start-up time. So, the value of the equivalent duty cycle of the converter will not be much smaller than the maximum duty cycle value of the hard switching condition. So, the maximum value of r_{Line} in the system with soft-start will be a bit greater than that of the hard-switching system. Therefore, the model based on the hard-switching condition shown in Fig. 6 and the corresponding criterion given in inequality (14) is still effective in providing a sufficient criterion to ensure stability under large-signal disturbance.

Fig. 10 shows the transient waveforms of the system obtained by the full-circuit simulation when S_{l2} is turned on some time after S_{l1} is turned on. Here, all the subsystems adopt the soft-start routine and the equivalent duty cycle of B_2 in the start-up process is adjusted to be equal to 0.79. According to Fig. 9, the stability boundary of the system under large-signal disturbance is $r_{\mathrm{Line}} \leq 0.91\ \Omega$. In Fig. 10(a), it can be observed that the whole system cannot maintain stable operation after B_2 is connected to the DC bus if the value of r_{Line} fail to satisfy the stability criterion. However, if the stability criterion can be satisfied, as shown in Fig. 10(b), after B_2 is connected to the DC bus, the system may undergo the adjusting transition and the system can recover to the normal operating region. It can be found that the full-circuit simulation results verify the effectiveness of the proposed criterion.

IV. Experimental Verification

A DC distribution system with one source converter (B_s) and two load converters (B_1 and B_2) is used to demonstrate the criterion proposed in Section III. Here, the topologies, the control methods and the parameters of B_1, B_2 and B_s are the same with the full-circuit simulation circuits shown in Section II. The maximum duty cycles of these three converters are 0.9. The input voltage (E) is 24 V and the values of r_{Line} and L_{Line} are 0.6 Ω and 5 μH, respectively, which account for the wire impedance from B_s to B_1 and B_2.

A. Hard Switching Subsystems Verification

Firstly, S_{l1} is turned on and both B_1 and B_s were stable before $t = 0$ s, and S_{l2} is turned on at $t = 0$ s. Substituting the parameters given in Table I into the inequality (14), we get $r_{\mathrm{Line}} \leq \min\{0.68\ \Omega, 0.54\ \Omega\}$. Hence, if r_{Line} is greater than 0.54 Ω, the system will lose stability under large disturbance.

Fig. 11(a) shows the transient waveforms of the system with $r_{\mathrm{Line}} = 0.6\ \Omega$ and $L_{\mathrm{Line}} = 5\ \mu$H. From Fig. 11(a), it can be observed that v_{bus} can be kept at the regulated value after B_2 is connected to the DC bus. However, v_{o1} drops to 5 V and v_{o2} can only reach the value of 25 V instead of its regulated value (30 V), and the system can be regraded as operating in a new orbit. However, the steady-state values of the output voltage on this orbit (5 V for B_1 and 25 V for B_2) are not the desired operating points. Therefore, the system is unstable under large-signal disturbance and a saddle-node bifurcation occurs. Moreover, the instability cannot be removed unless the system is shut down manually. When the system has $r_{\mathrm{Line}} = 0.5\ \Omega < 0.54\ \Omega$, which satisfies the proposed criterion, the system can operate normally after B_2 is connected to the DC bus, as shown in Fig. 11(b). The experimental results are in good agreement with the full-circuit simulation results, bifurcation analysis results, and also verify the effectiveness of the concept of the proposed criterion that the system's large-

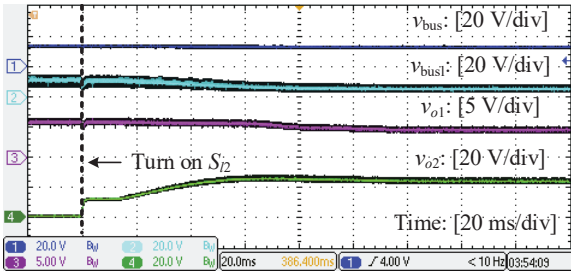

(a)

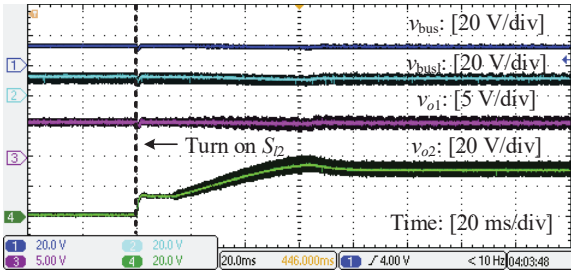

(b)

Fig. 12. Transient waveforms (a) for $r_{\rm Line} = 1\ \Omega$ (with soft-start), showing unstable system under large-signal disturbance; (b) for $r_{\rm Line} = 0.8\ \Omega$ (with soft-start), showing stable system under large-signal disturbance.

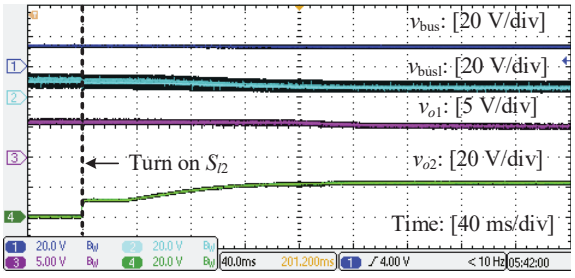

Fig. 13. Transient waveforms for $r_{\rm Line} = 0.7\ \Omega$ (with soft-start and the equivalent maximum duty cycle is about 0.7), showing unstable system under large-signal disturbance.

signal disturbance can be predicted by investigating the steady-state value of the input voltage of the load converters.

B. Soft-Start Switching Subsystems Verification

In the closed-loop controlled system with soft-start routine, however, the duty cycle of B_2 increases slowly after B_2 is plugged to the DC bus. Fig. 12(a) shows the system which includes a soft-start routine with $r_{\rm Line} = 1\ \Omega$ and $L_{\rm Line} = 5\ \mu$H. Initially, S_{l1} is on and S_{l2} is off. After converters B_1 and B_s have reached their steady states, S_{l2} is turned on. According to Fig. 8, when the system adopts soft-start, and the equivalent duty cycle of B_2 in the start-up process is adjusted to be equal to 0.79, if $r_{\rm Line} > 0.91\ \Omega$, the system will lose stability under large-signal disturbance. From Fig. 12(a), it can be observed that $v_{\rm bus}$ can be kept at the regulated value after B_2 is connected to the DC bus, but v_{o2} cannot reach its regulated value of 30 V and v_{o1} collapses and cannot recover to its normal operating region. Fig. 12(b) shows the same system with $r_{\rm Line} = 0.8\ \Omega$. It can be found that the system can operate normally after B_2 is connected to the DC bus, verifying the effectiveness of the proposed criterion on predicting the stability condition of the system with soft-start routine under large-signal disturbance.

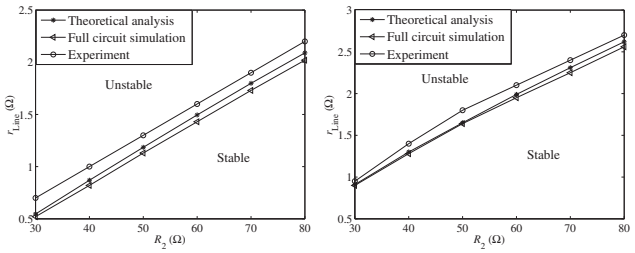

(a) (b)

Fig. 14. Operating boundaries for the system in $(R_2, r_{\rm Line})$ parameter space (a) without and (b) with soft-start.

According to the proposed criterion and Fig. 9, it can be found that the maximum value of $r_{\rm Line}$ will decrease if we increase the soft-start duration to limit the equivalent duty cycle of B_2 in the start-up process to below 0.79. Here, we adjust the soft-start parameters to set the equivalent duty cycle of B_2 to about 0.7. It can be predicted that the system is unstable under large-signal disturbance if $r_{\rm Line} = 0.7\ \Omega$. Fig. 13 shows the experimental result. It can be observed that B_1 cannot recover to its original operating region while B_2 cannot reach its desired operating point. This agrees with the prediction based on the proposed criterion.

C. Stability Boundary of the system

Stable transient operating boundaries in the $(R_2, r_{\rm Line})$ parameter space are compared with the theoretical analysis, as shown in Fig. 12. The boundary of the theoretical analysis shown in Fig. 14(a) can be obtained by varying the value of R_2 and calculating the results according to inequality (14). In Fig. 14(b), it can be obtained by varying the value of R_2, substituting the duty cycle value of B_2 from 0 to the maximum value in inequality (14) and plotting the relationship between D_{m2} and $r_{\rm Line}$ like the Fig. 9, and finding out the maximum value of$r_{\rm Line}$. In Fig. 14, the stable regions corresponding to the system can operate at the desired region under large-signal disturbance, while the unstable regions correspond to the system working in an undesirable operating regions under large-signal disturbance. It can be found that the results of the experiment and the full-circuit simulation are in good agreement with the theoretical analysis.

V. Conclusion

A bifurcation phenomenon has been found for the DC cascaded power system with multi-load converters. Essentially, the input voltage of the load converters collapses suddenly when an extra load converter connected to a non-ideal DC bus of the system. The root cause of this phenomenon is the saturation of the duty cycles of the load converters and the existence of the wire resistance of the DC bus. The voltage dropped across on the wire resistance may cause the input

voltage of the load converters to go below the permissible minimum value and the duty cycles of the load converters will be fixed at the maximum value. In this situation, the load converters fail to maintain the constant power load characteristic and behave as resistive loads. In addition, the output voltages of the load converters drop due to the saturation of duty cycles. Thus, the system cannot operate at the desired operating point, signifying an instability has occurred under large-signal disturbance. A common practice of improving the system's stability performance under this situation is to introduce the soft-start control. Stability boundaries have been identified for the system, clearly suggesting how the large-signal stability of the system could be affected by the variation of some selected parameters.

In this paper, we report an instability phenomenon in the DC distribution system and identify the cause of the instability. The physical origin of the unstable phenomenon is exposed through the bifurcation analysis. By investigating the adjusting transition and the stable operation requirements of the system under large-signal disturbance, a simple and effective large-signal criterion is proposed. The concept of the proposed criterion is that the large-signal stability of the system can be judged by investigating the DC operating point of the load converters' input voltage and the detailed dynamics of the system can be omitted. The proposed criterion can be extended to apply in large-scale DC distribution systems. In addition, the effect of the soft-start control is also taken into consideration in the proposed criterion, and the analytical results show that the proposed criterion can also predict the large-signal stability of the system with soft-start control and provide a sufficient criterion to guarantee the system's stability under large-signal disturbance. The results are presented in design-oriented forms to facilitate the identification of the parameter range that ensures system's stability under large-signal disturbance.

REFERENCES

[1] S. Luo and I. Batarseh, "A review of distributed power systems part I: DC distributed power system," *IEEE Aerosp. Electron. Syst. Mag.*, vol. 20, DOI 10.1109/MAES.2005.1499272, no. 8, pp. 5–16, Aug. 2005.

[2] S. Luo and I. Batarseh, "A review of distributed power systems Part II. high frequency AC distributed power systems," *IEEE Aerosp. Electron. Syst. Mag.*, vol. 21, DOI 10.1109/MAES.2006.1662037, no. 6, pp. 5–14, Jun. 2006.

[3] R. Haroun, A. Cid-Pastor, A. El Aroudi, and L. Martinez-Salamero, "Synthesis of canonical elements for power processing in dc distribution systems using cascaded converters and sliding-mode control," *IEEE Trans. Power Electron.*, vol. 29, DOI 10.1109/TPEL.2013.2261093, no. 3, pp. 1366–1381, Mar. 2014.

[4] A. Riccobono and E. Santi, "Comprehensive review of stability criteria for dc power distribution systems," *IEEE Trans. Ind. Appl.*, vol. 50, DOI 10.1109/TIA.2014.2309800, no. 5, pp. 3525–3535, May 2014.

[5] S. Liu, P. X. Liu, and X. Wang, "Stability analysis of grid-interfacing inverter control in distribution systems with multiple photovoltaic-based distributed generators," *IEEE Trans. Ind. Electron.*, vol. 63, DOI 10.1109/TIE.2016.2592864, no. 12, pp. 7339–7348, May 2016.

[6] S. Singh, A. R. Gautam, and D. Fulwani, "Constant power loads and their effects in dc distributed power systems: A review," *Renew. Sustain. Energy Rev.*, vol. 72, DOI 10.1016/j.rser.2017.01.027, pp. 407–421, Jan. 2017.

[7] R. D. Middlebrook, "Input filter considerations in design and application of switching regulators," in *Proc. IEEE IEEE IAS Annual Meeting*, 1976, pp. 366-382

[8] S. Schulz, B. Cho, and F. Lee, "Design considerations for a distributed power system," in *Proc. IEEE Power Electron. Spec. Conf.*, San Antonio, TX, DOI 10.1109/PESC.1990.131244, pp. 611–617, Jun. 1990.

[9] C. M. Wildrick, F. C. Lee, B. H. Cho, and B. Choi, "A method of defining the load impedance specification for a stable distributed power system," *IEEE Trans. Power Electron.*, vol. 10, DOI 10.1109/63.387992, no. 3, pp. 280–285, May 1995.

[10] P. Huynh and B. H. Cho, "A new methodology for the stability analysis of large-scale power electronics systems," *IEEE Trans. Circ. Syst. I, Fund. Theory Appl.*, vol. 45, DOI 10.1109/81.669060, no. 4, pp. 377–385, Apr. 1998.

[11] X. Feng, J. Liu, and F. C. Lee, "Impedance specifications for stable DC distributed power systems," *IEEE Trans. Power Electron.*, vol. 17, DOI 10.1109/63.988825, no. 2, pp. 157–162, Feb. 2002.

[12] S. Vesti, T. Suntio, J. Oliver, R. Prieto, and J. Cobos, "Impedance-based stability and transient-performance assessment applying maximum peak criteria," *IEEE Trans. Power Electron.*, vol. 28, DOI 10.1109/TPEL.2012.2220157, no. 5, pp. 2099–2104, May 2013.

[13] C. Rivetta and G. A. Williamson, "Large-signal analysis of a dc-dc buck power converter operating with constant power load," in *Proc. IEEE Ind. Electron. Soc. Meeting*, vol. 1. DOI 10.1109/IECON.2003.1280073, pp. 732–737, Nov. 2003.

[14] C. Rivetta and G. A. Williamson, "Global behaviour analysis of a dc-dc boost power converter operating with constant power load," in *Proc. IEEE Int. Symp. Circ. Syst.,* vol. 5, DOI 10.1109/ISCAS.2004.1329968, pp. 956–959, May 2004.

[15] F. Zhang and Y. Yan, "Start-up process and step response of a dc–dc converter loaded by constant power loads," *IEEE Trans. Ind. Electron.*, vol. 58, DOI 10.1109/TIE.2010.2045316, no. 1, pp. 298–304, Jan. 2011.

[16] F. Umbría, J. Aracil, and F. Gordillo, "Singular perturbation stability analysis of three phase two-level power converters," in *Proc. 18th Mediterr. Conf. Control Autom. (MED)*, Marrakesh, Morocco, DOI 10.1109/MED.2010.5547605, pp. 123–128, Jun. 2010.

[17] F. S. Garcia, J. A. Pomilio, G. S. Deaecto, and J. C. Geromel, "Analysis and control of dc-dc converters based on lyapunov stability theory," in *Proc. IEEE Energy Convers. Congr. Expo. (ECCE)*, DOI 10.1109/ECCE.2009.5316085, pp. 2920–2927, Sep. 2009.

[18] D. Marx, P. Magne, B. Nahid-Mobarakeh, S. Pierfederici, and B. Davat, "Large signal stability analysis tools in dc power systems with constant power loads and variable power loads-a review," *IEEE Trans. Power Electron.*, vol. 27, DOI 10.1109/TPEL.2011.2170202, no. 4, pp. 1773–1787, Apr. 2012.

[19] R. K. Brayton and J. K. Moser, "A theory of nonlinear networks-I," *Quart. Appl. Math.*, vol. 22, no. 1, pp. 1–33, 1964.

[20] L. Weiss, W. Mathis, and L. Trajkovic, "A generalization of Brayton-Moser's mixed potential function," *IEEE Trans. Circ. Syst. I, Fund. Theory Appl.*, vol. 45, DOI 10.1109/81.669065, no. 4, pp. 423–427, Apr. 1998.

[21] M. Huang, H. Ji, J. Sun, L. Wei, and X. Zha, "Bifurcation-based stability analysis of photovoltaic-battery hybrid power system," *IEEE J. Emerging Sel. Topics Power Electron.*, vol. 5, DOI 10.1109/JESTPE.2017.2681125, no. 3, pp. 1055–1067, Sep. 2017.

[22] W. Du, J. Zhang, Y. Zhang, and Z. Qian, "Stability criterion for cascaded system with constant power load," *IEEE Trans. Power Electron.*, vol. 28, DOI 10.1109/TPEL.2012.2211619, no. 4, pp. 1843–1851, Apr. 2012.

[23] X. Liu, Y. Zhou, W. Zhang, and S. Ma, "Stability criteria for constant power loads with multistage *LC* filters," *IEEE Trans. Veh. Technol.*, vol. 60, DOI 10.1109/TVT.2011.2148133, no. 5, pp. 2042–2049, Jun. 2011.

[24] C. K. Tse, *Complex behavior of switching power converters*. Boca Raton, FL, USA: CRC press, 2003.

[25] Y. Chen, C. K. Tse, S. S. Qiu, L. Lindenmüller, and W. Schwarz, "Coexisting fast-scale and slow-scale instability in current-mode controlled DC/DC converters: Analysis, simulation and experimental results." *IEEE Trans. Circ. Syst. I, Reg. Papers*, vol. 55, DOI 10.1109/TCSI.2008.923282, no. 10, pp. 3335–3348, Nov. 2008.

[26] P. Griffith, "Designing switching voltage regulators with the TL494," *Texas Instruments Application Report.* Available: http://focus. ti. com/lit/an/slva001d/slva001d. pdf, 2005.

Li Ding (Student Member) received the B.E. degree in information engineering from the Guangdong University of Technology, Guangzhou, China, in 2011, the M.E. degree in signal and information processing from the South China University of Technology, Guangzhou, in 2014.

He is currently pursuing the Ph.D. degree in power electronics with the Hong Kong Polytechnic University, Hong Kong. His current research interests include modeling and analysis power electronic systems and study the complex behavior in power electronic circuits.

Chi K. Tse (M'90–SM'97–F'06) received the BEng (Hons) degree with first class honors in electrical engineering and the PhD degree from the University of Melbourne, Australia, in 1987 and 1991, respectively.

He is presently Chair Professor of Electrical Engineering at City University of Hong Kong, Hong Kong. Prior to joining City University of Hong Kong in October 2019, he was with Hong Kong Polytechnic University, with which he served as Head of the Department of Electronic and Information Engineering from 2005 to 2012. His research interests include power electronics, nonlinear systems and complex network applications. He was awarded a number of research and industry awards, including Prize Paper Awards by IEEE TRANSACTIONS ON POWER ELECTRONICS in 2001, 2015 and 2017, RISP Journal of Signal Processing Best Paper Award in 2014, Best paper Award by International Journal of Circuit Theory and Applications in 2003, two Gold Medals at the International Inventions Exhibition in Geneva in 2009 and 2013, a Silver Medal at the International Invention Innovation Competition in Canada in 2016, a Grand Prize and Gold Medal at the Silicon Valley International Invention Festival in 2019, and a number of recognitions by the academic and research communities, including honorary professorship by several Chinese and Australian universities, Chang Jiang Scholar Chair Professorship, IEEE Distinguished Lectureship, Distinguished Research Fellowship by the University of Calgary, Gledden Fellowship and International Distinguished Professorship-at-Large by the University of Western Australia. While with the Hong Kong Polytechnic University, he received the President's Award for Outstanding Research Performance twice, Faculty Research Grant Achievement Award twice, Faculty Best Researcher Award, and several teaching awards.

Dr. Tse serves and has served as Editor-in-Chief for the IEEE TRANSACTIONS ON CIRCUITS AND SYSTEMS II (2016-2019), *IEEE Circuits and Systems Magazine* (2012-2015), Editor-in-Chief of *IEEE Circuits and Systems Society Newsletter* (since 2007), Associate Editor for three IEEE Journal/Transactions, Editor for *International Journal of Circuit Theory and Applications*, and is on the editorial boards of a few other journals. He currently chairs the steering committee for the IEEE Transactions on Network Science and Engineering. He also serves as panel member of Hong Kong Research Grants Council, and member of several professional and government committees.